

Crystallization kinetics and growth mechanism of $\text{Pb}(\text{Zr}_{0.52}\text{Ti}_{0.48})\text{O}_3$ nanopowders

Mohammad Khajelakzay · Ehsan Taheri-Nassaj

Received: 22 February 2014 / Accepted: 24 March 2014 / Published online: 6 April 2014
© Springer-Verlag Berlin Heidelberg 2014

Abstract In this study, $\text{Pb}(\text{Zr}_{0.52}\text{Ti}_{0.48})\text{O}_3$ nanopowders were synthesized via sol–gel process. Particle morphology, crystalline phases and thermal behavior were characterized by scanning electron microscopy, X-ray diffraction and simultaneous thermal analyzer, respectively. The X-ray diffraction pattern showed perovskite phase clearly. The non-isothermal activation energy for the perovskite crystallization in $\text{Pb}(\text{Zr}_{0.52}\text{Ti}_{0.48})\text{O}_3$ gel powders was $224.91 \text{ kJ mol}^{-1}$. Both growth morphology parameter (n) and crystallization mechanism index (m) are close to 3.0, indicating that the bulk nucleation is dominant in the perovskite PZT formation. To determine dielectric properties, the calcined $\text{Pb}(\text{Zr}_{0.52}\text{Ti}_{0.48})\text{O}_3$ nanopowders were pressed using uniaxial press. It was found that the $\text{Pb}(\text{Zr}_{0.52}\text{Ti}_{0.48})\text{O}_3$ disks, by sintering at $1,200 \text{ }^\circ\text{C}$ for 2 and 10 h, and at 1 kHz frequency, had 966 and 1,490 of the dielectric constant, respectively.

1 Introduction

Lead zirconate titanate, $\text{Pb}(\text{Zr}_x\text{Ti}_{1-x})\text{O}_3$ (PZT), piezoelectric ceramics with a composition close to the morphotropic phase boundary (MPB) ($x = 0.52\text{--}0.55$) exhibit a large dielectric constant, a high spontaneous polarization, and a great piezoelectric response [1, 2]. Dielectric and piezoelectric properties of PZT are related to the

tetragonal-rhombohedral phase transition composition. This transition is frequently categorized as morphotropic because it corresponds to a structural change with the variation in composition [3]. PZT thin-film and powders have been synthesized through sol–gel [4], metallo-organic decomposition (MOD) [5, 6], reactive calcinations [7], coprecipitation [8], ball milling [9], hydrothermal reaction [10] and others [11, 12]. Among the chemical methods, the sol–gel processing is remarkable due to the advantages of high purity and homogeneity of the nanopowder. In addition, the preparation takes place at a relatively low temperature, not exceeding $600 \text{ }^\circ\text{C}$. Also because the mixing is accomplished in solution, the components are mixed on the atomic scale in a relatively short time. PZT-based materials can be found in numerous applications including hydrophones, fish finders, ultrasonic transducers, sensors and actuators, etc. [13].

The thermal behavior of various materials has been investigated by a DTA technique. For the crystallization and phase transition study of materials, DTA is useful in determining the transformation temperature [14–16].

The sol–gel method has been extensively used to prepare single-phase nano-crystalline PZT powders and ceramics, thin films, fibers, etc. [17–19]. This study aims to synthesize perovskite lead zirconate titanate nanopowders with ultra-fine dimensions of about 7 nm and to investigate the phase transformation, growth mechanism, crystallization kinetics, their dielectric constant (ϵ_r) and dielectric loss ($\tan\delta$).

2 Experimental procedure

Lead (II) acetate tri-hydrate ($\text{Pb}(\text{CH}_3\text{CO}_2)_2 \cdot 3\text{H}_2\text{O}$, Merck), zirconium *n*-propoxide (70 wt% solution in 1-propanol,

M. Khajelakzay (✉)
Department of Materials Science and Engineering, Malek Ashtar
University, Isfahan, Iran
e-mail: m.khajelakzay@gmail.com

E. Taheri-Nassaj
Department of Materials Science and Engineering, Tarbiat
Modares University, Tehran, Iran

Zr[OCH(CH₃)₂]₄, Merck) and titanium iso-propoxide (Ti[OCH(CH₃)₂]₄, Merck) were used as the starting materials to introduce the Pb, Zr, and Ti cations into the solution in a 1:0.52:0.48 ratio, respectively. 2-Methoxy ethanol (CH₃OCH₂CH₂OH, Merck) was introduced as a solvent and stabilizer for zirconium and titanium precursors and lead acetate tri-hydrate. The sol was dried at 90 °C until a transparent resinous xerogel was formed. The gel was dried at 100 °C for 2 days, and then calcined in different temperatures for 1 h [20, 21]. The phase analysis of the PZT powders was characterized by X-ray Diffraction (XRD; Philips X-Pert X-ray diffractometer with Cu K α radiation at 40 kV) analysis.

Cohen's method of determining lattice parameters is more valuable when applied to non-cubic substances [22]. In this investigation, it was used form 11 planes between $2\theta = 20\text{--}70^\circ$ [(001), (100), (101), (110), (111), (002), (200), (102), (201), (112) and (211)], and then, used the method of Least Squares. For tetragonal crystal structure:

$$\sin^2 \theta_{\text{true}} = \frac{\lambda^2}{4} \times \left(\frac{h^2 + k^2}{a^2} + \frac{l^2}{c^2} \right) \quad (1)$$

where:

$$\sin^2 \theta - \frac{\lambda^2(h^2 + k^2)}{4a^2} - \frac{\lambda^2(l^2)}{4c^2} = -2K \sin \theta \cos^2 \theta \quad (2)$$

By rearranging this equation and introducing new symbols, we obtain:

$$\sin^2 \theta = C\alpha + B\gamma + A\delta \quad (3)$$

where:

$$C = \frac{\lambda^2}{4a^2}, \quad \alpha = h^2 + k^2, \quad B = \frac{\lambda^2}{4c^2}, \quad \gamma = l^2, \\ A = -2K, \quad \text{and} \quad \delta = \sin \theta \cos^2 \theta.$$

The values of C , B , and A , of which only the first two are really needed, are found from the three normal equations:

$$\sum \alpha \sin^2 \theta = C \sum \alpha^2 + B \sum \alpha\gamma + A \sum \alpha\delta \quad (4)$$

$$\sum \gamma \sin^2 \theta = C \sum \alpha\gamma + B \sum \gamma^2 + A \sum \gamma\delta \quad (5)$$

$$\sum \delta \sin^2 \theta = C \sum \alpha\delta + B \sum \delta\gamma + A \sum \delta^2 \quad (6)$$

Simultaneous Thermal Analysis (STA 1640) was used to identify the crucial steps in the pyrolysis and calcination processes, from room temperature to 900 °C, with a heating rate of 5–40 °C/min in air atmosphere. The grain size and morphology were assessed using a High Resolution Transmission Electron Microscope (HR-TEM Philips CM30—150 kV). To determine dielectric properties, first, the calcined PZT nanopowders were pressed using uniaxial press, under a pressure of 80 MPa to form discs with the diameter of 10 mm and thickness of about 1 mm; then the

PZT pellets were sintered in air for 2, 10 h at 1,200 °C, with the heating rate being fixed at 5, 10, 20, 30 and 40 K/min.

The electrodes were polished and then covered with silver suspension containing the organic solvent. Electrodes were also formed in the oven after 10 min at 110 °C. The dielectric constants and dielectric loss ($\tan\delta$) were measured with the LCR Meter (GW Instek-800 Series) using a constant frequency of 1, 10 and 100 kHz.

3 Results and discussion

3.1 Thermal behavior and phase formation

Figure 1 shows the results of thermo gravimetric analysis, TGA, and differential thermal analysis, DTA, with a heating rate of 5 K min⁻¹. From the TGA pattern, a large amount of weight loss was observed at 423 and 467 °C. These temperatures seem to be critical in the sintering of the PZT gel. Below 250 °C, the weight loss was shown in the TGA curve and the weak broad endothermic DTA peak was due to the evaporation of the volatile solvent. Between 300 and 500 °C, the weight loss was due to the removal and decomposition of organic groups [23, 24]. Two DTA peaks around 423 and 467 °C correspond to a weaker and a stronger exothermic DTA peaks. The former may have resulted from decomposition Precursors of organic material and the latter, from PbO formation [24]. There was a weak exothermic peak in the DTA curve around 512 °C which is related to the formation of the perovskite phase [25]. The horizontal curves of TG–DTA were achieved around 600 °C, indicating that the complete formation of the perovskite PZT nanopowders was achieved at a furnace temperature greater than 600 °C. The X-ray diffraction

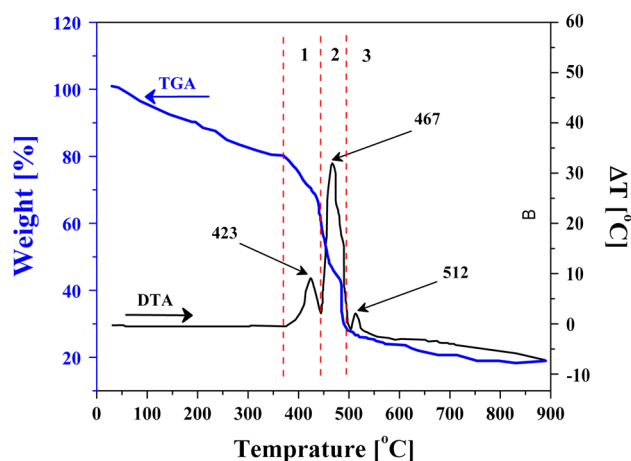


Fig. 1 Thermal gravity and derivation analysis (TG–DTA) of dried gel of PZT

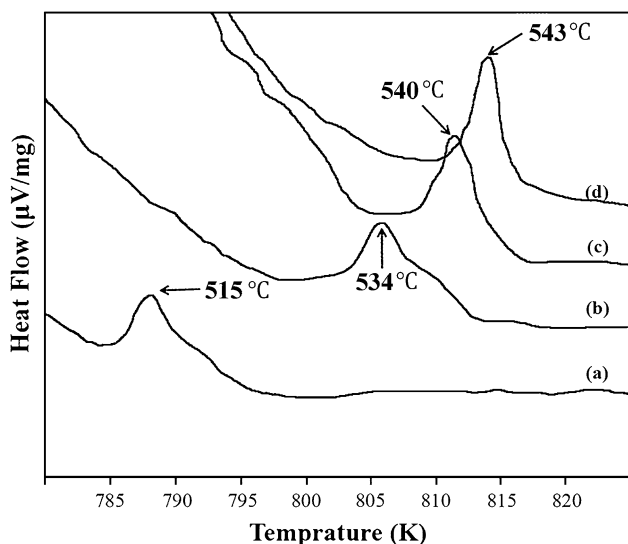


Fig. 2 Exothermic peak of DTA curves for PZT gel powders at various heating rates: **a** 10, **b** 20, **c** 30 and **d** 40 K min⁻¹

showed that the perovskite structures were formed at around 600 °C, corresponding well with the TG–DTA results.

The crystallization kinetics of the PZT nanopowders were compared using DTA analysis at different heating rates. Figure 2 shows the DTA curves for the crystallization of the PZT gel powders at various heating rates, B , ranging from 10 to 40 K min⁻¹. It was found that the exothermic peak was shifted to a higher temperature when the heating rate was increased. When the heating rate was increased, the rearrangement was delayed to the high temperature side.

The XRD patterns of PZT gel powders obtained at various temperatures are shown in Fig. 3. Pyrochlore phase ($\text{Pb}_2\text{Ti}_2\text{O}_6$) peaks began to appear in 400 °C (Fig. 3a), starting transformation into PZT at 500 °C (Fig. 3b). The latter continued to grow until 600 °C (Fig. 3c), at which all peaks were identified as PZT peaks. The XRD pattern of PZT powder heat treated at 600 °C exhibited broad peaks indicative of fine crystalline particles. The PZT average crystallite size was calculated to be approximately 6 nm using Modified Scherrer's equation:

$$\ln B = \ln(K\lambda/T) + \ln(1/\cos \theta_B) \quad (7)$$

where λ is the X-ray wavelength in nanometer (nm), B is the peak width of the diffraction peak profile at half maximum height resulting from small crystallite size in radians and K is a constant related to crystallite shape, normally taken as 0.9 [13]. The XRD results also showed the existence of a perovskite phase for the PZT nanopowders prepared by the sol–gel method for all temperatures. This result agrees well with the DTA measurement, which showed that the crystallization process was

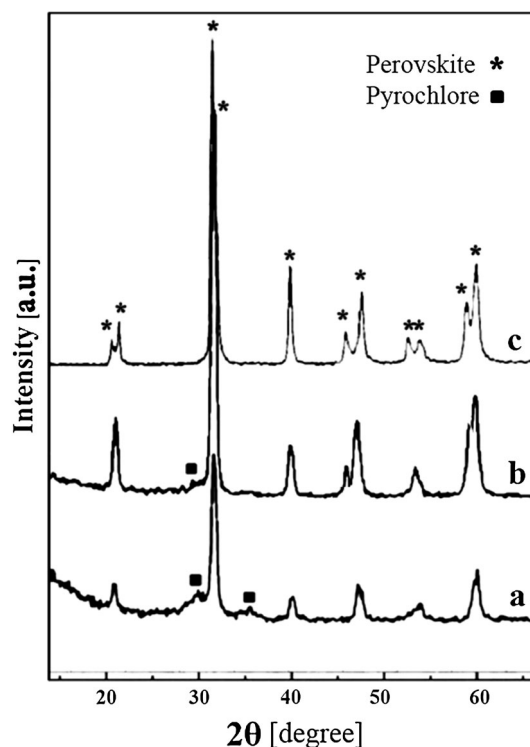


Fig. 3 X-ray diffraction patterns of lead zirconate titanate nanopowders calcined at: **a** 400 °C, **b** 500 °C and **c** 600 °C

completed at about 600 °C. The low temperature perovskite crystallization can be ascribed to the decomposition and combustion of the organic complexes. The lattice parameters were determined by Cohen's method from the XRD pattern at 600 °C. In the tetragonal crystal structure, lattice parameters (a and c) were obtained 0.4039 and 0.4148 nm, respectively. These values are agreed with PDF card 33-0784, very well ($a = 0.40360$ and $c = 0.41460$ nm).

3.2 Crystallization kinetics

The exothermic peak of DTA curve shows that the crystallization temperature (T_c) and the temperature depend on the heating rate (B), which is represented by the Arrhenius equation [14]. In order to calculate the activation energy of perovskite crystallization in PZT gel powders, the Johnson–Mehl–Avrami (JMA) equation [26] can be used:

$$\ln B = -E_c/RT_c + \ln CM \quad (8)$$

where E_c is the apparent crystallization activation energy, R represents the universal gas constant and $\ln CM$ is a constant. From the DTA curves at different heating rates, a linear relation is achieved between $\ln B$ and $1/T_c$ as shown in Fig. 4. Thus, the apparent activation energy was obtained from the slope of the fitted straight line, namely, 224.91 kJ mol⁻¹. This result is smaller than 295–494 kJ mol⁻¹, which is

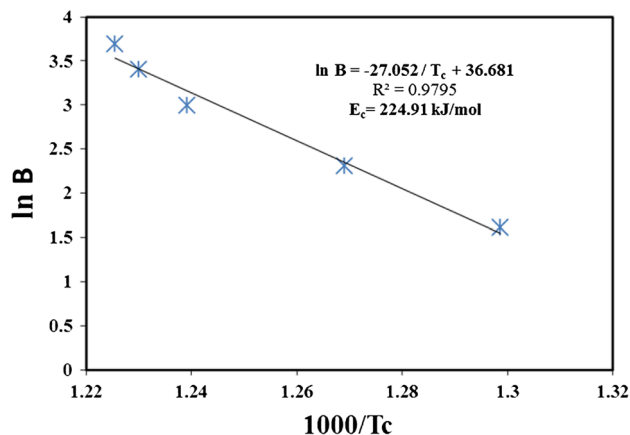


Fig. 4 Plots of $\ln B$ vs. $1000/T_c$

reported in the literature [27]. This difference can be attributed to the various precursor materials and manufacture processes that have different chemical homogeneities in PZT polycrystals crystallization [28, 29].

The HR-TEM image of PZT nanopowder calcinated at 600 °C, and its particle size distribution are shown in Fig. 5a, b. The figure shows that the PZT nanopowders exhibit a narrow distribution and are nearly spherical in morphology. From HR-TEM images, the average particle size of PZT nanopowders (Fig. 5b) was found to be about 7.3 nm in diameter (with Image Analyzer Program).

The dielectric constant can be calculated by determining the capacitance of the pellets having electrodes that cover the major surfaces. By employing the LCR Meter, the capacitance of the samples can be calculated according to IEEE Standard [30]. After obtaining the capacitance, relative dielectric constant can be calculated using plate condenser:

$$C = (\epsilon_r \cdot \epsilon \cdot S) / d \quad (9)$$

where S is the area of the specimen, d is the thickness of the specimen, and ϵ is the vacuum dielectric constant ($\epsilon = 58.855 \times 10^{-12}$ F/m). Table 1 show that the dielectric constant depends on the sintering time and the frequency. It

Table 1 The ϵ_r and $\tan \sigma$ of the sintered PZT pellets

Sintering Conditions	Frequency (kHz)	ϵ_r	$\tan \sigma$
1,200 °C, 2 h	1	966	0.06
	10	907	0.09
	100	883	0.17
1,200 °C, 10 h	1	1,490	0.009
	10	1,242	0.05
	100	1,021	0.14

was seen that the ϵ_r was decreased and the $\tan \delta$ was increased with increasing frequency (Table 1). It was understood that at higher frequencies, a space charge polarization from conducting ions at the interface could not follow the change of the electric field, thereby leading to a non-ferroelectric appearance [31–34]. The ϵ_r was increased with an increase in sintering time because the PZT grain size was increased with an increase in sintering time [3, 13, 34].

3.3 Growth mechanism of the perovskite PZT formation

When a sample is crystallized in a DTA run, the exothermic peak is related to the growth morphology parameter (n). A higher value of n means a narrower peak. The DTA curve shows a narrower peak at a higher heating rate of 40 K min⁻¹ as shown in Fig. 2. The simplified Johnson–Mehl–Avrami (JMA) expression is:

$$\log [-\ln (1 - \alpha)] = -m \cdot \log B - (n \cdot E_c / 2.303 RT) + \text{constant} \quad (10)$$

where n means the growth morphology parameter, and m denotes the crystallization mechanism index. For the bulk nucleation and constant number of nuclei such as the three-dimensional growth, $m = 3$ and $n = 3$. For the two-dimensional growth, $m = 2$ and $n = 2$. For $m = n = 1$, it describes one-dimensional growth or surface nucleation from a constant number of nuclei [35]. The calculated value of n decreases with increasing heating rate as listed in

Fig. 5 HR-TEM micrograph of the prepared PZT nanopowders at calcination temperatures of 600 °C for 1 h

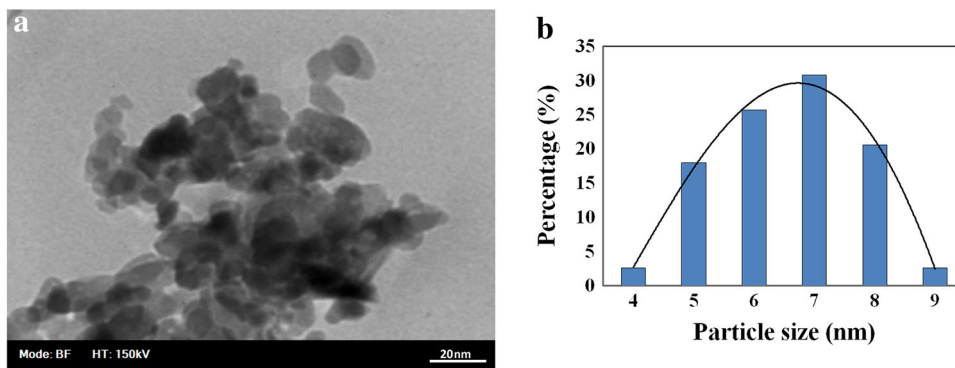


Table 2 Growth morphology parameters of n and m at various heating rates and temperatures

Heating rate (K min ⁻¹)	nE_c (kJ mol ⁻¹)	n	m
10	739.95	3.29	2.73
20	717.46	3.19	2.65
30	694.97	3.09	2.69
40	631.99	2.81	2.53
Average	696.09	3.09	2.65

Table 2. It is found that n is 3.29 at a heating rate of 10 K min⁻¹ and decreases gradually to 2.81 as the heating rate increases to 40 K min⁻¹, in which the initial crystallization mechanism is characterized by instantaneous nucleation. Within an experimental error, the average value is approximated to 3. The non-isothermal result with a reaction order n of 3 for the perovskite PZT formation in the PZT gel powders can be estimated. According to the JMA criterion, $n = 3$ describes three dimensional growth from a constant number of nuclei and shows a spherical-like morphology [36, 37], that has been examined by HR-TEM in Figs. 5.

According to Eq. (4), m value could be determined and listed in Table 2. Those values are also approximately 3. These results also indicate that the bulk nucleation is dominant in the perovskite PZT crystallization and the crystal growth is controlled by diffusion at a fixed number of nuclei in the PZT gel powders.

4 Conclusions

Powder samples were prepared by sol–gel method, and for dielectric properties measurement, pellet samples were prepared via uniaxial pressing and sintering at 1,200 °C, for 2 and 10 h. STA analysis showed that the crystalline phase was fully up to temperature of 600 °C and the non-isothermal activation energy for the perovskite crystallization in PZT gel powders was 224.91 kJ mol⁻¹. The X-ray diffraction showed that the perovskite structures were formed at around 600 °C, corresponding well with the TG–DTA results. The PZT average crystallite size was calculated to be approximately 6 nm. The obtained lattice parameters agree with PDF card 33-0784, very well. According to the JMA criterion, $n = 3$ describes three dimensional growth from a constant number of nuclei and shows a spherical-like morphology, and $m = 3$ indicate that the bulk nucleation is dominant in the perovskite PZT crystallization and the crystal growth is controlled by diffusion at a fixed number of nuclei in the PZT gel powders. From HR-TEM images, the average particle size of PZT nanopowders was found to be about 7.3 nm in diameter. In terms of dielectric properties, It was found that the ϵ_r was

decreased and the $\tan\delta$ was increased with an increase in frequency and a decrease in sintering time.

References

- J.F. Tressler, S. Alkoy, R.E. Newnham, *J. Electroceram.* **2**, 257 (1998)
- A.J. Moulson, J.M. Herbert, *Electroceramics: materials, properties, applications* (Wiley, New York, 2003)
- M. Soares, A. Senos, P. Mantas, *J. Eur. Ceram. Soc.* **20**, 321 (2000)
- V. Palkar, M. Multani, *Mater. Res. Bull.* **14**, 1353 (1979)
- J. Fukushima, K. Kodaira, T. Matsushita, *J. Mater. Sci.* **19**, 595 (1984)
- S.Y. Chen, I.W. Chen, *J. Am. Ceram. Soc.* **81**, 97 (1998)
- C.A. Randall, N. Kim, J.P. Kucera, W. Cao, T.R. Shrout, *J. Am. Ceram. Soc.* **81**, 677 (1998)
- K.R. Mohana Rao, A. Rao, S. Komarneni, *Mater. Lett.* **28**, 463 (1996)
- L. Kong, W. Zhu, O. Tan, *Mater. Lett.* **42**, 232 (2000)
- T. Kutty, R. Balachandran, *Mater. Res. Bull.* **19**, 1479 (1984)
- T. Yamamoto, *Am. Ceram. Soc. Bull.* **71**, 978 (1992)
- N. Chakrabarti, H. Maiti, *Mater. Lett.* **30**, 169 (1997)
- A. Monshi, M.R. Foroughi, M.R. Monshi, *World. J. NanoSci. Eng.* **2**, 154 (2012)
- K. Matusita, T. Komatsu, R. Yokota, *J. Mater. Sci.* **19**, 291 (1984)
- J. MacDowell, G. Beall, *J. Am. Ceram. Soc.* **52**, 17 (1969)
- J.H. Simmons, Uhlmann, G.H. Beall, *Nucleation and crystallization in glasses* (American Ceramic Society, USA, 1981)
- A. Wu, I.M.M. Salvado, P.M. Vilarinho, J.L. Baptista, *J. Am. Ceram. Soc.* **81**, 2640 (1998)
- G. Yi, Z. Wu, M. Sayer, *J. Appl. Phys.* **64**, 2717 (1988)
- R. Meyer, T. Shrout, S. Yoshikawa, *J. Am. Ceram. Soc.* **81**, 861 (1998)
- M. Khajelakzay, E. Taheri-Nassaj, *Mater. Lett.* **75**, 61 (2012)
- M. Khajelakzay, E. Taheri-Nassaj, *Electron. Mater. Lett.* **10**, 4 (2013)
- B.D. Cullity, *Am. J. Phys.* **25**, 394 (1957)
- M. Khajelakzay, E. Taheri-Nassaj, in *Proceeding of the 3rd International Conference on Ultrafine Grained and Nanostructured Materials* (Tehran, 2011)
- J. S. A. Y. Wang, *Carbon and PZT Nanofibers through Electrospinning* (USA, 2011)
- S.Y. Chen, I.W. Chen, *J. Am. Ceram. Soc.* **77**, 2337 (1994)
- A. Marotta, A. Buri, *Thermochim. Acta* **25**, 155 (1978)
- O. Babushkin, T. Lindbäck, K. Brooks, N. Setter, *J. Eur. Ceram. Soc.* **17**, 813 (1997)
- P. Durán, J. Tartaj, J.F. Fernández, M. Villegas, C. Moure, *Ceram. Int.* **25**, 125 (1999)
- Y.-F. Chen, M.-C. Wang, M.-H. Hon, *J. Eur. Ceram. Soc.* **24**, 2389 (2004)
- T. Furukawa, J. Fujino, E. Fukada, *Jpn. J. Appl. Phys.* **15**, 2119 (1976)
- Z. Li, H. Gong, Y. Zhang, *Curr. Appl. Phys.* **9**, 588 (2009)
- A. Chaipanich, N. Jaitanong, R. Yimnirun, *Ferroelectr. Lett.* **36**, 59 (2009)
- Q. Zhao, D. Su, M. Cao, G. He, J. Di, J. Yuan, D. Wang, *J. Mater. Sci. Mater. El* **24**, 3521 (2013)
- G.S. Wang, D. Rémiens, E. Dogheche, R. Herdier, X.L. Dong, *J. Am. Ceram. Soc.* **89**, 3417 (2006)
- D.W. Henderson, *J. Therm. Anal. Calorim.* **15**, 325 (1979)
- C.-S. Hsi, M.-C. Wang, *J. Mater. Res.* **13**, 2655 (1998)
- G. He, G. Chen, Z. Bian, *Intermetallics* **8**, 481 (2000)